



UNIVERSIDADE ESTADUAL DE CAMPINAS
SISTEMA DE BIBLIOTECAS DA UNICAMP
REPOSITÓRIO DA PRODUÇÃO CIENTÍFICA E INTELLECTUAL DA UNICAMP

Versão do arquivo anexado / Version of attached file:

Versão do Editor / Published Version

Mais informações no site da editora / Further information on publisher's website:

<https://onlinelibrary.wiley.com/doi/10.1111/aor.12671>

DOI: 10.1111/aor.12671

Direitos autorais / Publisher's copyright statement:

©2016 by Wiley. All rights reserved.

DIRETORIA DE TRATAMENTO DA INFORMAÇÃO

Cidade Universitária Zeferino Vaz Barão Geraldo

CEP 13083-970 – Campinas SP

Fone: (19) 3521-6493

<http://www.repositorio.unicamp.br>



Bilaminar Device of Poly(Lactic-co-Glycolic Acid)/Collagen Cultured With Adipose-Derived Stem Cells for Dermal Regeneration

*Juliana A. Domingues, †Giselle Cherutti, ‡Adriana C. Motta, §Moema A. Hausen, ‡Rômulo T.D. Oliveira, §Elaine C.M. Silva-Zacarin, ‡Maria Lourdes P. Barbo, and †‡Eliana A.R. Duek

**Department of Cell Biology and Structural, Biology Institute; †Department of Materials Engineering, Faculty of Mechanical Engineering, UNICAMP, Campinas; ‡Department of Physiological Sciences, Biomaterials Laboratory, PUC- SP; and §Department of Biology, Structural Biology Laboratory, UFSCAR, Sorocaba, Brazil*

Abstract: Several materials are commercially available as substitutes for skin. However, new strategies are needed to improve the treatment of skin wounds. In this study, we developed and characterized a new device consisting of poly(lactic-co-glycolic acid) (PLGA) and collagen associated with mesenchymal stem cells derived from human adipose tissue. To develop the bilaminar device, we initially obtained a membrane of PLGA by dissolving the copolymer in chloroform and then produced a collagen type I scaffold by freeze-drying. The materials were characterized physically by gel permeation chromatography, scanning electron microscopy, and mass loss. Biological activity was assessed by cell proliferation assay. A preliminary study in vivo was performed with a pig model in which tissue regeneration was assessed macroscopically and histologically, the commercial device Integra being used as a

control. The PLGA/collagen bilaminar material was porous, hydrolytically degradable, and compatible with skin growth. The polymer complex allowed cell adhesion and proliferation, making it a potentially useful cell carrier. In addition, the transparency of the material allowed monitoring of the lesion when the dressings were changed. Xenogeneic mesenchymal cells cultured on the device (PLGA/collagen/ASC) showed a reduced granulomatous reaction to bovine collagen, down-regulation of α -SMA, enhancement in the number of neoformed blood vessels, and collagen organization as compared with normal skin; the device was superior to other materials tested (PLGA/collagen and Integra) in its ability to stimulate the formation of new cutaneous tissue. **Key Words:** Collagen scaffold—Dermal—Mesenchymal stem cells—Poly(lactic-co-glycolic acid)—Tissue regeneration.

Individuals with extensive skin lesions (e.g., full-thickness burns) suffer a substantial loss of dermis that does not regenerate spontaneously and may require a skin graft (1,2). Over the years, skin regeneration has been attempted with various types of transplantation, such as xenografts, allografts, or autografts. However, antigenicity (in allografts and xenografts) and the limited number of donor sites available (in autografts) mean that in many cases,

these substitutes are unsuccessful in promoting skin regeneration (3,4). Hence, there is a need to develop devices that can adequately replace the damaged tissue (5).

Several commercially available materials are used as substitutes for skin, including Integra, a three-dimensional (3D) porous matrix made up of type I collagen associated to glycosaminoglycan (GAG) as a dermal equivalent and a silicone layer to simulate the epidermal portion that must subsequently be removed (6,7), and Dermagraft, a synthetic polymer of poly(lactic-co-glycolic acid) (PLGA) that is used as a dermal substitute and over which human fibroblasts derived from newborn foreskin can be cultivated. In general, bioresorbable material provides a suitable support for the proliferation and secretion of

doi:10.1111/aor.12671

Received July 2015; revised September 2015.

Address correspondence and reprint requests to Dr. Eliana A. R. Duek, Laboratório de Biomateriais, Faculdade de Ciências Médicas e da Saúde PUC/SP, Rua Joubert Wey, 290, Sorocaba, São Paulo CEP18030-070, Brasil. E-mail: eliduek@pucsp.br

extracellular matrix (8). PLGA is approved by the United States Food and Drug Administration for use in humans and provides good cellular adhesion and proliferation (9); polymer degradation occurs through cleavage of its ester bonds and by generation of products that are excreted in the urine or metabolized by conventional pathways (10).

The requirements that must be met in the development of a suitable dermal substitute are considerable and include the ability to protect the wound from infection and fluid loss, easy handling, and good resistance (11). Desirable properties of scaffolds include the provision of mechanical support, regulation of cellular activities, support and definition of 3D tissue organization, and maintenance of a normal state of differentiation (12). The use of collagen in tissue engineering is well documented as in Yannas and Burke where the first scaffold composed of collagen and GAG is described (13). A scaffold of collagen provides structural space for accommodation, proliferation, and migration of fibroblasts and endothelial cells, in addition to allowing nutrient exchange between the material and the environment (14).

Recently, artificial scaffolds for cutaneous lesions have been combined with stem cells in order to improve skin regeneration (15). Adipose-derived stem cells (ASCs) have emerged as an attractive candidate for wound healing, as they can accelerate healing by producing bioactive substances that decrease inflammation in the wound and accelerate the formation of new vessels and granulation tissue (16). ASCs have been associated with reduced formation of fibrosis, for regulating both collagen deposition by fibroblasts and their conversion to myofibroblasts (17). Myofibroblasts are cells characterized by the expression of alpha-smooth muscle actin (α -SMA) with a contractile phenotype and related to fibrosis formation (18). Drugs with anti-scarring effect reduce the conversion of fibroblasts to myofibroblasts and promote a balance between the synthesis and degradation of collagen which reduces the formation of fibrosis (19,20).

In this study, we developed a bilaminar device consisting of PLGA and collagen type I cultured with human adipose mesenchymal cells. The innermost layer of the device proved to be porous and allowed the adhesion, spreading, proliferation, and invasion of ASCs. However, the outer layer was found to be dense, which reduced the loss of water and invasion by micro-organisms, and was bioresorbable, remaining in the lesion only for the time required for formation of granulation tissue. When implanted in pigs, this device enhanced formation of new skin com-

pared with other materials without ASCs. Our results indicate the potential of this device for use in situations when prevention of infection and reduction of scarring are necessary.

MATERIALS AND METHODS

Device preparation

The PLGA (80:20) used to obtain the membrane was synthesized at the Laboratory of Biomaterials, School of Medical Sciences and Health, PUC/SP, Brazil, according to Motta (21), and had a high molar mass (Mw 315 000 g/mol). PLGA membranes were prepared by dissolving the copolymer to a concentration of 5% (w/v) in chloroform (CHCl_3) at room temperature. To make the scaffold, a solution of bovine skin collagen (6 mg/mL) and 1-ethyl-3-[3-dimethylaminopropyl] (EDC) was used. The solution was frozen at -20°C for 24 h and lyophilized. For cross-linking, the scaffold was placed in a solution of 95% ethanol in water (pH 7.0) supplemented with 50 mM EDC. The scaffold was washed 10 times with distilled water to remove residual EDC.

In vitro degradation test

The device was immersed in 10 mL of phosphate-buffered saline (PBS) and incubated at 37°C . After 7, 14, 21, and 28 days of incubation, samples were recovered and washed 10 times with distilled water. The in vitro degradation of PLGA membranes was monitored by gel permeation chromatography (GPC). The average molecular weight (Mw) was obtained by GPC CLWA-1 at 25°C with THF (tetrahydrofuran, 10 mg/mL) as the mobile phase. The columns used were polystyrene 10^2 , 10^4 , and 10^5 together with a Waters 410 refractive index detector (Waters Corporation, Milford, MA, USA). The degradation of collagen scaffold was obtained for weight loss.

Scanning electron microscopy (SEM)

The sample of the PLGA/collagen device (obtained in liquid nitrogen) was fractured, and surfaces of PLGA and collagen were coated with gold (Sputter Coater BAL-TEC SCD 050, Capovani Brothers, Inc., Scotia, NY, USA) and examined in a JEOL JXA 860 scanning electron microscope (Zeiss, Oberkochen, Germany) operated at 10 kV.

Proliferation and morphology of ASCs on the device

The human ASCs used in this experiment were kindly provided by Dr. Sara Teresinha Olalla Saad (Department of Clinical Medicine, Faculty of Medical Sciences, State University of Campinas—

UNICAMP, Campinas, Brazil). For cell culture, collagen was sterilized with 70% ethanol for 1 h, washed with PBS, and maintained in DMEM without FBS for 24 h at 37°C in a CO₂ incubator. The proliferation and morphology of ASCs after culture on device were analyzed by laser scanning confocal microscopy (LSCM—Leica TCS SP8, Wetzlar, Germany). For this purpose, the medium was removed and cells fixed with a solution containing 4% (v/v) paraformaldehyde in 0.1 M phosphate buffer, pH 7.4. For morphology evaluation, the samples were washed with PBS, permeabilized with Triton-X 100, and incubated with Alexa Fluor 647 phalloidin (Invitrogen) (200 units/mL) and with DAPI. The cell proliferation assay was performed after 1, 5 and 10 days of culture in the device. To this end, the nuclei of the cells were stained with DAPI and counted by the 3D images obtained. The 3D reconstruction was performed after obtaining the total rebuilding focal planes in 100 µm thickness starting from the surface of the material which received the cells; for each sample ($n = 3$), four random fields were chosen.

In vivo study in a porcine model

A Large White pig (~20 kg) was fasted for 12 h before use. Initially an intramuscular injection of ketamine (20 mg/kg) and xylazine (2 mg/kg) was given, followed by surgical anesthesia with propofol (0.29 mg.kg⁻¹.min⁻¹). Six full-thickness lesions (3 cm in diameter) were created on the dorsum, two for each treatment. After the injury, the commercial product Integra (control), PLGA/collagen, and PLGA/collagen/cell devices were implanted. In the immediate post-operative period, an intravenous injection of tramadol (2 mg/kg) and during the experimentation period the same analgesic was mixed into the feed at a dose of 12 mg/kg every 24 h. On the 28th post-operative day, the animal was anesthetized as described above and laid on its side on a surgical table and sacrificed with thiopental (90 mg/mL, i.v.). Samples of the previously injured tissue were removed and fixed in 10% formalin for histological analysis followed by staining of sections with hematoxylin-eosin (HE) or Picrosirius Red to analyze the organization of collagen fibers (22) and Masson's trichrome for vessels quantification by the ImageJ software (23). The sections were examined with a Nikon Eclipse E800 microscope, sections stained with Picrosirius Red were visualized by wide-field polarized light microscopy, and images were captured with Image Pro-Plus software. This study was approved by the Committee for Ethics in Animal Use at UNESP/Botucatu (protocol no. 01246-2012).

Immunohistochemistry for myofibroblast detection

The analysis of alpha-SMA expression was performed on samples fixed in 4% formaldehyde and included in paraffin. Serial sections were incubated overnight with specific primary antibodies for anti-SMA (ab7817, Abcam, Cambridge, MA, USA) and amplified using MACH4 Systems, according to the manufacturer's protocol (Biocare Medical, Concord, CA, USA). Color development was carried out with a 3,3'-diaminobenzidine solution and counterstained with hematoxylin. Reactions were subjected to quantitative analysis. In brief, each sample was analyzed by two independent observers with a light microscope (Nikon Eclipse E800, Nikon, Tokyo, Japan) equipped with a CCD camera (Nikon Digital Sight DS-Ri, Nikon) and high-resolution images (1280 × 1060 pixels) from three different random fields were taken. The images were analyzed with GSA Image Analyser Software (GSA Bansemer and Scheel GbR, Rostock, Germany). For the analysis, the area of positive reaction (brown-stained) was selected by color sampling in the software and converted into black pixels. The results were expressed as the mean of the positive area in mm².

Statistical analysis

Statistical analysis was done by using one way analysis of variance (ANOVA). Difference between groups was analyzed by Tukey test, $P < 0.05$ indicating significance (Prism version 6.03). Data were expressed as means ± standard deviation (SD), with $n = 3$.

RESULTS

In vitro degradation

The extent of degradation in vitro was determined separately for each material, at intervals of 7, 14, 21, and 28 days. Collagen degradation analysis was based on the loss of mass. The weight of collagen decreased over time after PBS incubation at 37°C and, after 28 days of degradation, approximately 20% of the original mass had been lost (Fig. 1A). Figure 1B shows the degradation of PLGA and the decrease in the average molecular weight in relation to the initial Mw during in vitro degradation assay. There was a marked decrease (~41%) in the molecular weight of the polymer after 7 days, with a more discrete reduction over the following 2 weeks. After 28 days, the decrease was ~70% compared with the initial molecular weight.

Scanning electron microscopy (SEM)

The morphology of the device was analyzed by SEM. The PLGA membrane was dense (Fig. 2A,C),

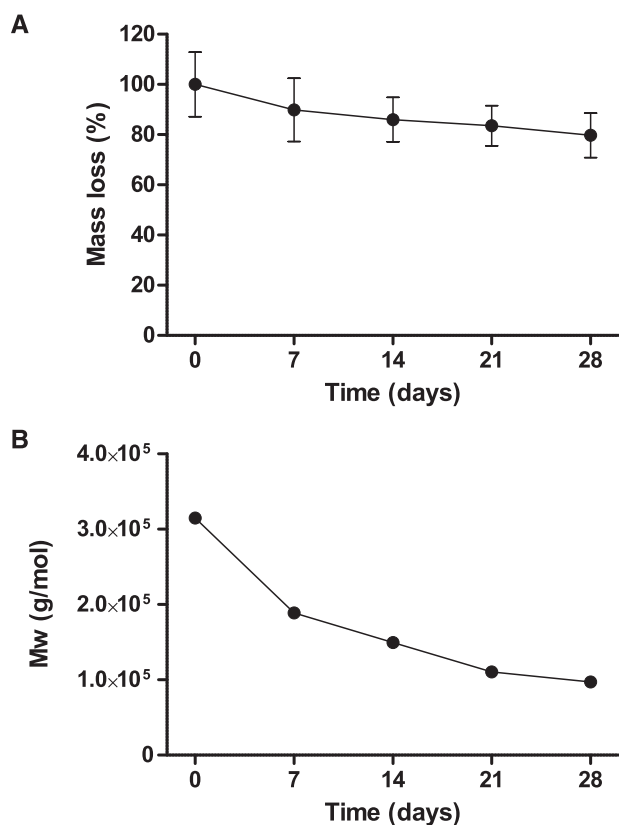


FIG. 1. In vitro degradation of device. Mass lost by the collagen scaffold as a function of time. All *P* values were > 0.05 (A). Change in the Mw of PLGA versus degradation time (B).

whereas the collagen scaffold had become extremely porous with pores approximately 100 μm in diameter (Fig. 2B,C).

Proliferation and morphology of ASCs on device

To determine if the collagen scaffold was compatible with cell growth, survival, and spreading, morphology and proliferation assays were performed with LSCM. After 24 h of culture, ASCs were present in the scaffold, between the collagen fibers with a spreading morphology (Fig. 3A–D). The proliferation assay of ASCs was performed after 1, 5, and 10 days of culture in collagen scaffolds. For this purpose, the nuclei of ACSs were stained with DAPI, and counting was performed after 3D reconstruction of the images. To analyze cell invasion, a 10-day culture scaffold (Fig. 3G) was used as a positive control to determine the maximum depth that could be detected. Our data showed that 150 μm is the maximum depth (data not shown) that cells soak in the scaffold. After reconstruction of all images, we saw that ASCs were able to migrate and proliferate into the collagen scaffold over time (Fig. 3E–H).

In vivo assessment of recovery from injury

The ability of the device to promote tissue regeneration was assessed in a porcine model of skin lesion in which portions of skin were surgically removed from the dorsum of the pig to produce a full-

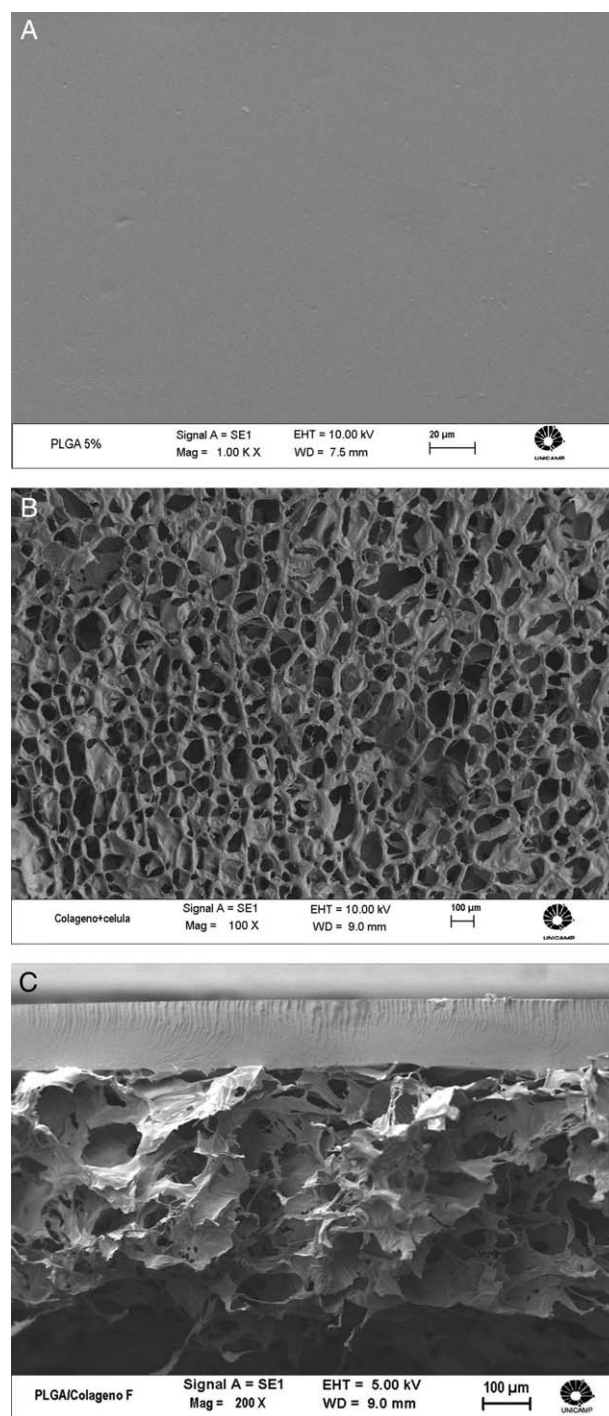


FIG. 2. Scanning electron micrographs of device. PLGA membrane surfaces (A). Collagen scaffold surface (B). Cross-section of device PLGA/collagen (C).

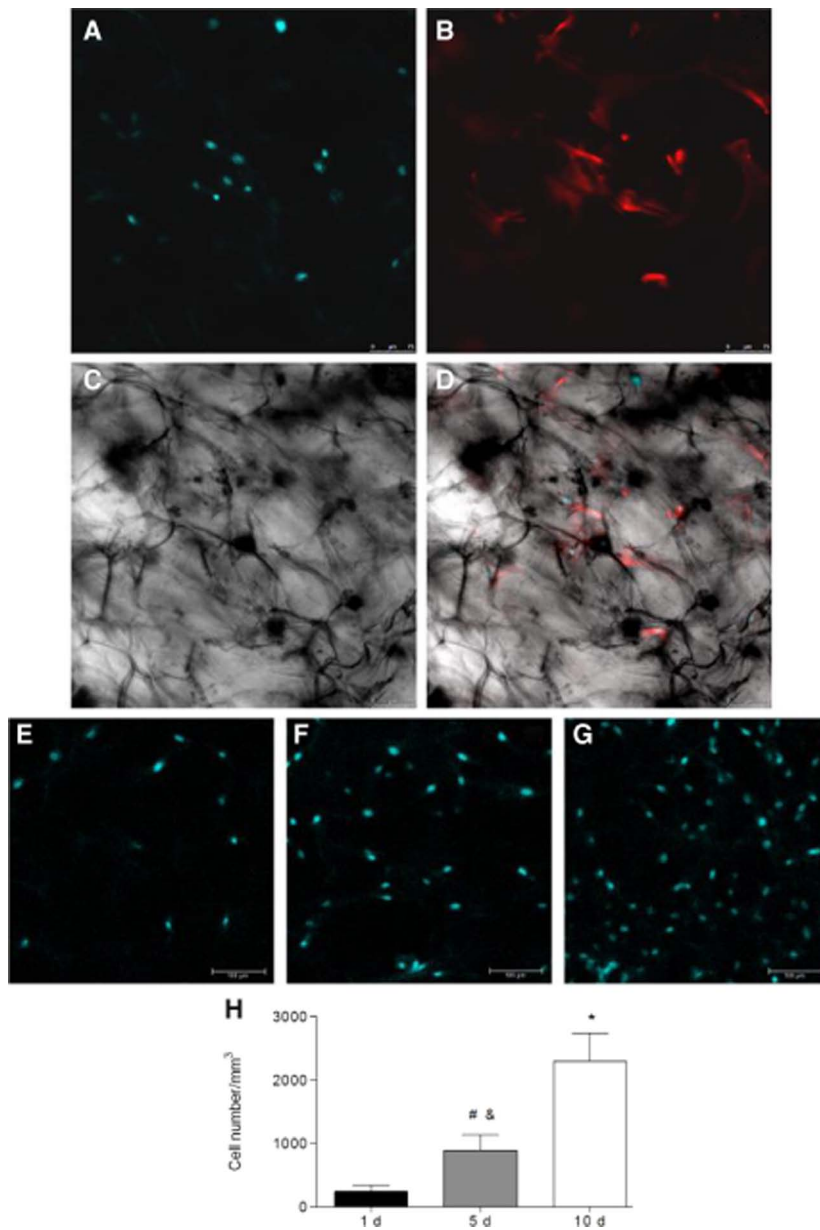


FIG. 3. Detection of ASC morphology and proliferation on collagen scaffold. Cell morphology and adhesion observed after culture for 24 h by identification of nuclei by DAPI staining (blue) (A); cytoplasm (red) with Alexa Fluor 647 dye conjugated to phalloidin (B); and through the confocal laser deflection, the collagen and porosity (black areas) were identified (C). Merged images (A, B, and C) identified the ASCs inside the material (D). Proliferation of ASCs occurred after 1, 5, and 10 days of culture (E, F, and G, respectively). Quantitative analyses of ASC proliferation (H): the columns represent the mean \pm SD ($n = 3$). Statistical significance of $P < 0.05$ (#1 vs. 5 days; &5 vs. 10 days; *1 vs. 10 days). Bars (A–D) 75 μm ; (E–G) 100 μm .

thickness injury (i.e., down to the muscle fascia). The implants were monitored and photographed after 7, 14, 21, and 28 days (Fig. 4). The membrane transparency allowed visual monitoring of lesion progression. There was no loss of implanted material and no sign of infection. On day 7, an inflammatory exudate was observed with all of the materials tested, and after 14 days, the silicone layers from the Integra implant and PLGA membranes were removed because the granulation tissue already appeared below these materials. The formation of granulation tissue was observed in all treatments.

Histological analysis

After 28 days, the skin with the implants was excised and examined for general and subcutaneous appearance, the presence of ulceration, the pattern of dermal collagen, and the presence of dermal and subcutaneous inflammatory infiltrate. Uninjured skin tissue was used for comparison (Fig. 5A,E). All groups showed granulation tissue formation. In the Integra group, there was presence of material not yet degraded, which may have led to extensive granulomatous inflammatory infiltrates (Fig. 5B,F). The PLGA/collagen group also presented inflamma-

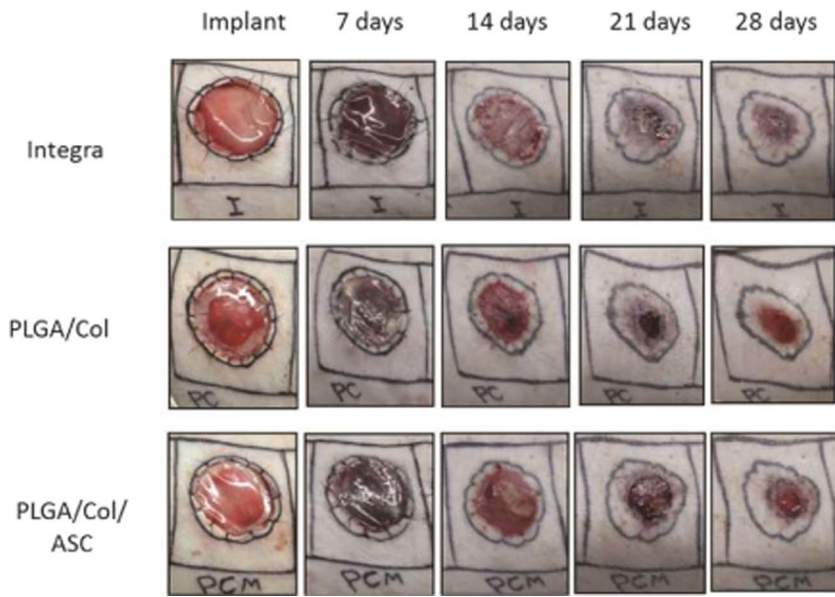


FIG. 4. Macroscopic lesion appearance. A pig model of skin injury was used. Small pieces of the skin were surgically removed and Integra, PLGA/Col, and PLGA/col/ASC were implanted. Lesions and implanted material appearance at 7, 14, 21, and 28 days.

tory infiltrate with foreign body granulomas (Fig. 5C); however, the group containing ASCs showed few granulomas (Fig. 5D). In addition, the pattern of collagen production was more similar between the normal skin and the device that contained ASCs (Fig. 6A vs. D and G) with a more complex collagen structure with collagen bundles distributed on multiple levels. Also, a greater amount of newly formed vessels was observed in the group containing ASCs (Fig. 7D,E).

Immunohistochemistry analysis

Sections of the wounds were stained with an antibody against α -SMA, useful for identifying myofibroblasts, a cellular group involved in the process of scar formation (18). After 21 days, sections provided from wounds implanted with Integra or PLGA/collagen (Fig. 8B,C,E) showed a large staining area (brown staining) for α -SMA; there was no statistical difference between these two treatments. This result indicates that the devices induced a wide

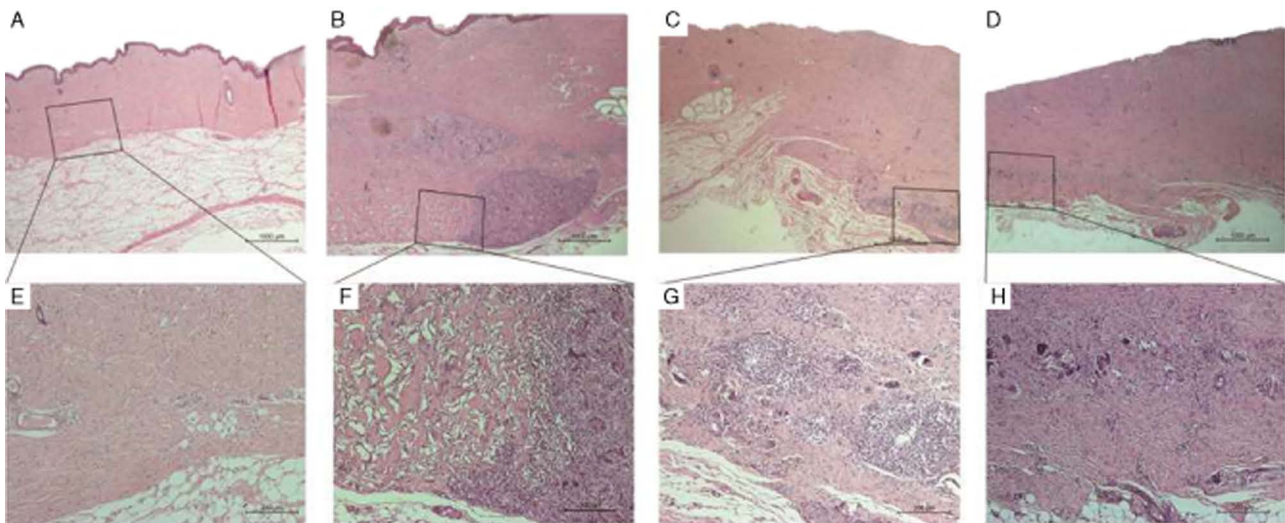


FIG. 5. Histological analysis of skin after hematoxylin and eosin staining. Uninjured skin, showing the normal epidermis, dermis, and hypodermis (A, E); Integra—re-epithelialized area and granulomatous inflammatory infiltrate between dermis and hypodermis (B, F). PLGA/col—interface between the dermis and hypodermis showing extensive inflammatory infiltrate with foreign body granulomas (C, G); PLGA/col/ASCs—small granulomas (D, H).

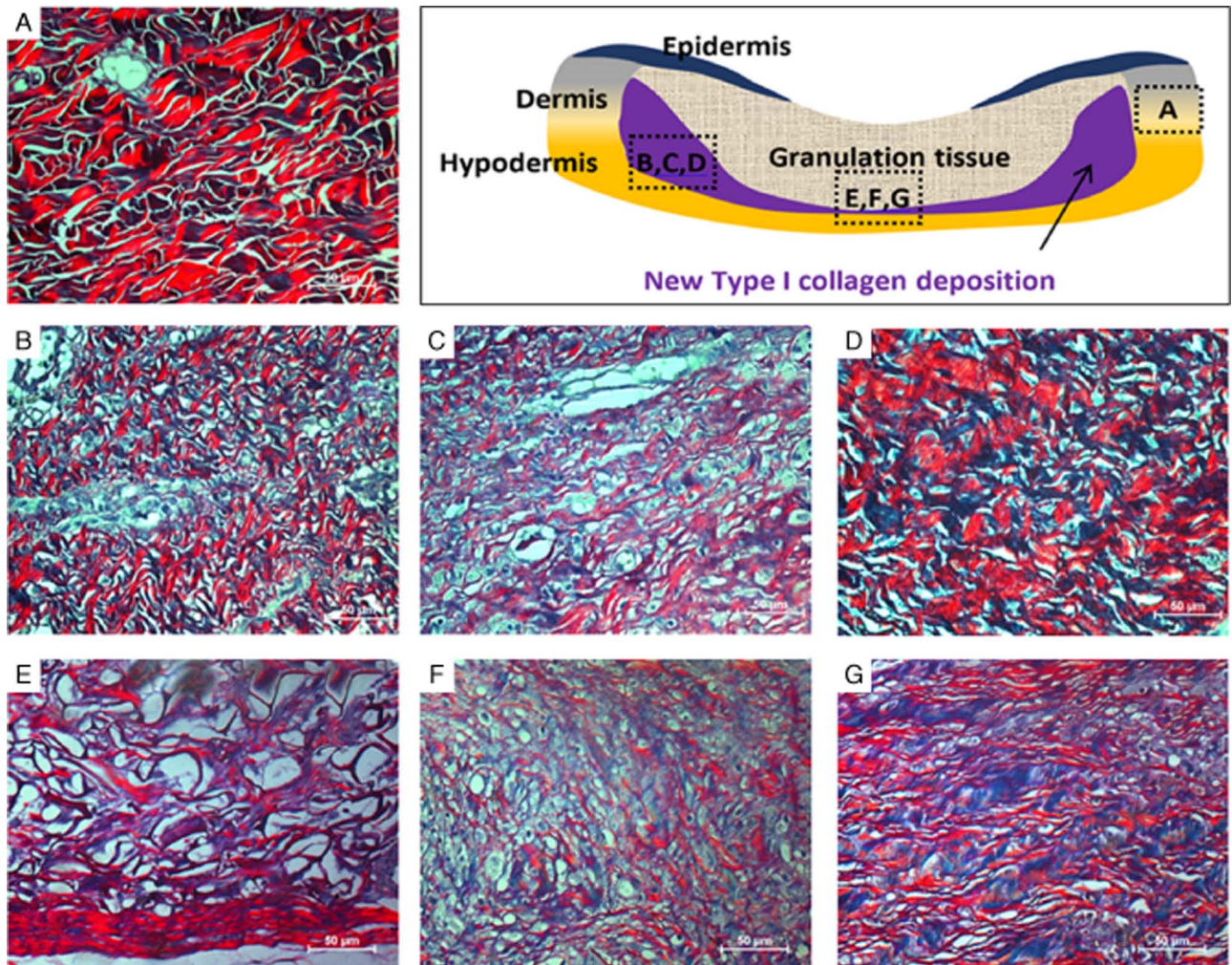


FIG. 6. Images of skin stained with Picrosirius Red showing the organization of the collagen fibers in different groups. A schematic transversal section is depicted for proper identification of the respective regions observed. Images (B, C, D) were obtained from a distal healing area as identified in the scheme, which has increased type I collagen deposition, while (E, F, G) images were obtained from a healing central area. The PLGA/col/ASC group presented a homogeneous deposition of type I collagen as compared with other groups. Uninjured skin (A); Integra (B, E); PLGA/col (C, F); and PLGA/col/ASCs (D,G).

formation of myofibroblasts. In contrast, when the implanted material contained ASCs (PLGA/col/ASC), the positive staining area for α -SMA was minimal (Fig. 8D,E), which suggests the induction of scarring was inhibited by the presence of ASCs. These results indicate that ASCs contributed to wound healing and diminished scar formation.

DISCUSSION

Several factors should be considered for developing a device as a skin substitute in tissue engineering, including pore size, biocompatibility, biodegradability, and regulation of fibrosis formation. In this study, a bilaminar device consisting of fully biodegradable and bioresorbable PLGA/collagen was developed.

This device was associated with ASCs to contribute to the neo-dermis formation via the production of cytokines and growth factors, as it has been shown that ASC alone has better capacity to induce regeneration of the skin than localized delivery of growth factors such as bFGF and EGF (24). Besides, devices for dermal regeneration must have the properties to keep hydration, avoid infection, and must improve dermal healing (25). As porous scaffolds favor wound repair (26), the collagen itself is an ideal scaffold that presents biological intrinsic compatibility and can be organized in porous networks. But, such collagen properties can cause its rapid dispersion through the grafted area and cannot avoid infection and dehydration. However, in this work, the PLGA was applied surrounding the collagen scaffold

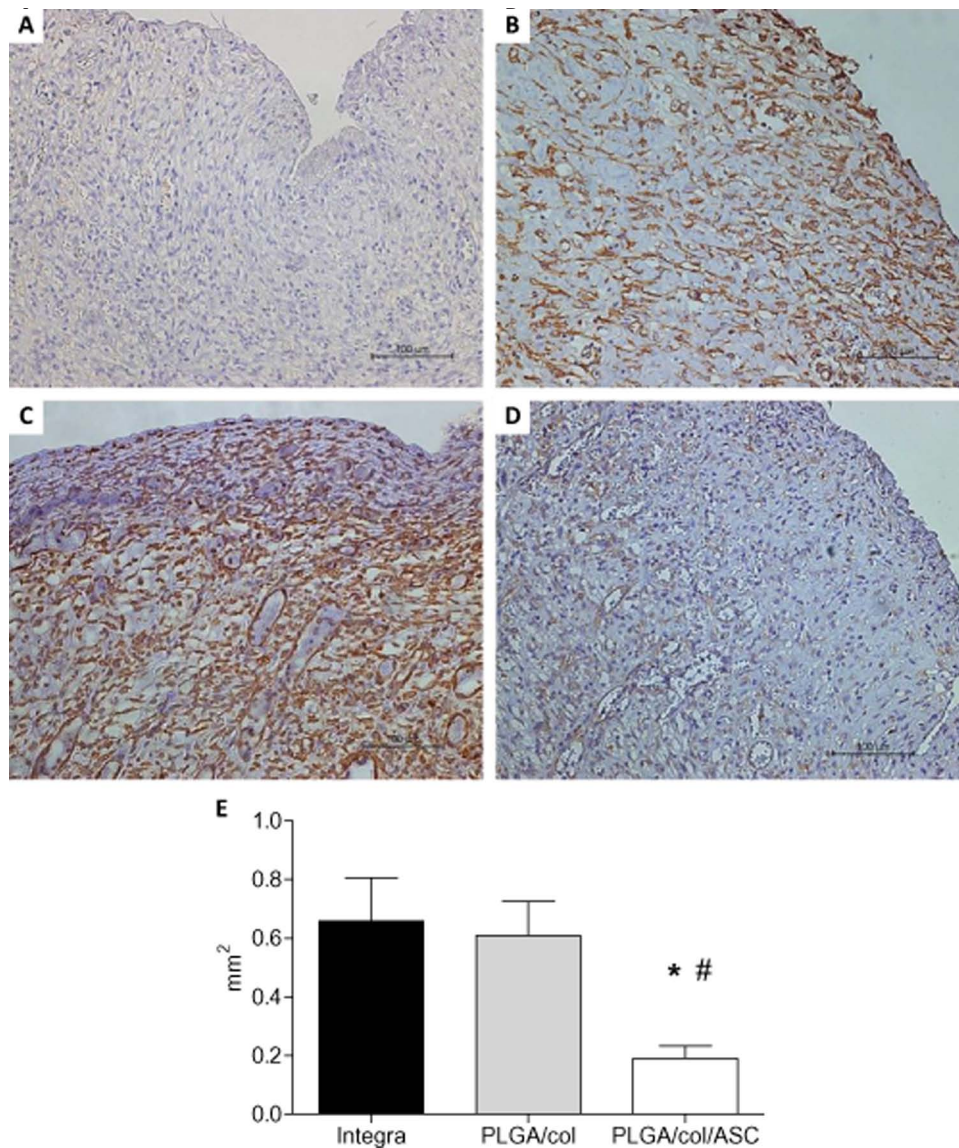


FIG. 7. Samples stained with Masson's trichrome for quantitative analysis of vessels in different groups. Uninjured skin (A); Integra (B); PLGA/col (C); and PLGA/col/ASCs (D). Number of vessels quantified by the ImageJ software (E). *# $P < 0.05$ (Integra vs. PLGA/col/ASC, and PLGA/col vs. PLGA/col/ASC, respectively).

adding to the device a holding support with an increased degradation curve, which maintains hydration as it also favors controlled collagen exposition avoiding its rapid dispersion. Additionally, it can also decrease the infection possibility as it acts as a physical barrier.

Degradation experiments showed that the PLGA membrane lost ~70% of its initial molecular weight after 28 days. Loss of mass is an important characteristic in developing materials to be used on skin as the material must degrade at a rate similar to that of organ growth. Compared with other bioabsorbable polymers, PLGA has a short degradation time (27),

and its low crystallinity facilitates hydration and hydrolysis (28). In contrast, analysis of collagen degradation in vitro showed only a small loss (20%) after 28 days, but this can be markedly accelerated in vivo by the action of collagenase. Some studies have used a collagenase solution to analyze collagen degradation (29), whereas others have used macrophages cultured in vitro (30). The in vivo study of this work shows that the collagen scaffold was completely degraded after 28 days of implantation.

Device biocompatibility is a requirement, but it is also important to have a porous 3D structure to allow the cell adhesion and growth required for

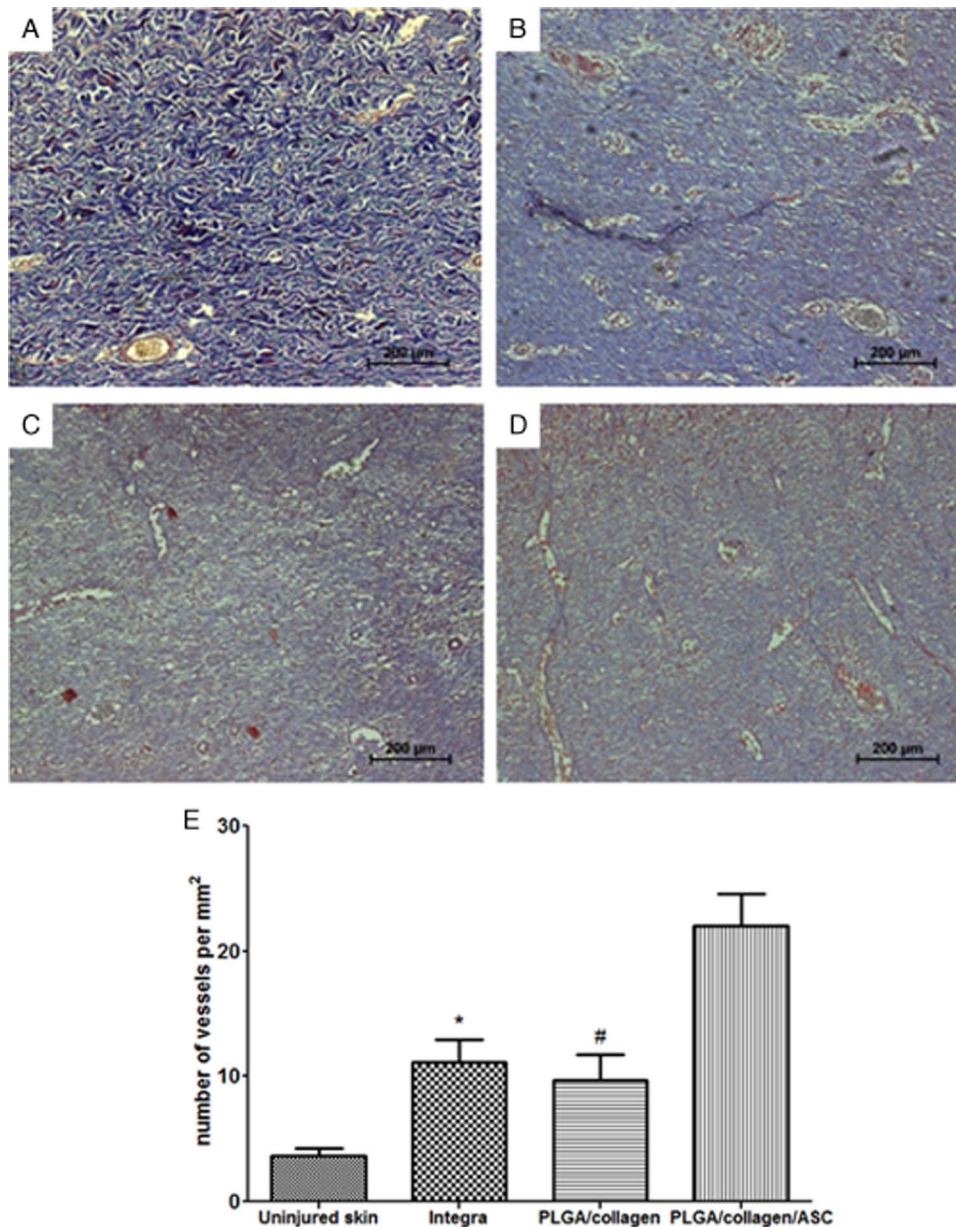


FIG. 8. Immunohistochemistry for α -SMA. For negative control, primary antibody was omitted (A). Positive staining for α -SMA in Integra (B), PLGA/col (C), and PLGA/col/ASC groups (D). Graphic demonstration of data obtained from positive staining area for α -SMA (E). * # $P < 0.05$ (Integra vs. PLGA/col/ASC, and PLGA/col vs. PLGA/col/ASC, respectively).

neovascularization (26,31). Angiogenesis on dermal substitutes is a major problem in wound repair in view of the importance of supplying oxygen and nutrients to cells at the wound site (32). The collagen scaffold developed here was entirely porous as observed by SEM, with regular pores of $\sim 100 \mu\text{m}$ in diameter, a size considered ideal for cellular infiltration and angiogenesis (33) and, in this case, it allowed cell adhesion, growth, and migration over deeper layers of the scaffold (approximately $150 \mu\text{m}$ deeper). Our preliminary results of SEM analysis of

the scaffold with cells in culture (data not shown) presented scarce cells adhered, but when confocal analysis was performed, it was observed that almost all cells had migrated through the scaffold pores. Cell migration through the scaffold was restricted to $150 \mu\text{m}$ at all culture times (1 to 10 days). Such boundary thickness in cell invasion could be attributed to oxygen and nutrient diffusion limitations of the medium flow through the scaffold pores. Such limitations were identified by Szot et al. (34) in a 3D model based on collagen I hydrogels for

tumoral growth. These authors reported that the limits for cell migration and viability in their model ranged from 150 to 200 μm inside the scaffold, while deeper cells were expressing hypoxic factors indicating cell death. As conventional cell culture models in scaffolds cannot be extrapolated to *in vivo* conditions for assorted purposes, but also due to striking differences in fluid flow through the scaffold. Such static conditions in this model probably restrict the maximum thickness for migration, and it has been reported (35) that bioreactors can improve oxygen and nutrient diffusion.

In this study, a porcine animal model was used because of its anatomical and physiological similarity to human skin (36). Full-thickness lesions (down to the muscle fascia) were produced on the dorsum of the animal. The commercial device Integra was used as a control, as it is structurally more similar to our device. Both have bovine collagen type I that usually induces a discrete inflammatory response, and presents an external cover layer of silicone for Integra or PLGA in our developed device. Other devices for skin healing, such as Dermagraft, were not supposed to be used in this work, as they have differentiated human cells which could induce a late rejection in xenogeneic transplants (37). When the Integra device was used, there was accentuated collagen deposition with a thick dermis, as well as irregular areas with a younger appearance and the presence of dense collagen. This profile indicated strong collagen deposition in the dermis. At the interface with the hypodermis, there was an extensive inflammatory reaction with two distinct patterns of granulomas: one containing giant cells surrounding confluent "empty" spaces and the other with granulomas containing multinucleated cells and a lymphocytic inflammatory infiltrate. Differently from the other groups, there were inflammatory foci in the reticular dermis, suggesting an attempt to eliminate foreign body material at the dermal-hypodermal interface. The deposition of collagen in the dermis or hypodermis was accentuated with the presence of myofibroblastic cells.

In PLGA/collagen membranes, there was a marked granulomatous reaction at the interface of the reticular dermis with the hypodermis and delayed maturation of dermal collagen, with no full wound closure in one of the segments. These findings suggest that, without the presence of progenitor cells, collagen is unable to stimulate the proper formation of new skin. In contrast, the combination of PLGA/collagen/ASCs was associated with small granulomas and foci of mononuclear cells. The less intense foreign body reaction in this

case compared with PLGA/collagen may reflect better healing and maturation of components associated with the dermis and hypodermis. The arrangement of collagen fibers was more similar to normal skin than in the other treatments. The exacerbated inflammatory response seen with the commercial device Integra and with the PLGA/collagen membrane was probably triggered by the bovine collagen of these samples as some authors have demonstrated the immunogenic capacity of this protein (38,39).

It is also known that mesenchymal stem cells produce growth factors such as VEGF and β -FGF that stimulate the neo-vascularization (40–42) process required for promoting wound maturation and healing (43). In this study, we observed a greater amount of newly formed vessels in the group containing ASCs as compared with the other groups tested. These results are in accordance with other studies that demonstrate the paracrine effect exercised by mesenchymal stem cells during wound healing (41,43).

Although inflammation was observed with the PLGA/collagen/ASCs device, this was less evident compared with the PLGA/collagen device, perhaps because of the immunoregulatory properties of mesenchymal stem cells (44,45) that can attenuate inflammation in the lesion. This property has led to the use of these cells to prevent and treat autoimmune diseases, and to reduce the rejection of allogeneic skin grafts (44). Liu et al. (46) demonstrated that the immunoregulatory properties of mesenchymal stem cells regulate scarring. It is suggested that ASCs modulate the expression of TGF- β 1 and TGF- β 3 (41). Hypertrophic scars are associated with overexpression of TGF- β 1, which promotes excessive deposition of collagen by fibroblasts and differentiation of these cells into myofibroblasts, resulting in formation and contraction of scars. The ASCs increased TGF- β 3 expression, which is known to inhibit scar formation and reduce expression of TGF- β 1 (47). Our results corroborate these studies as they have demonstrated less myofibroblast differentiation in device-associated ASCs.

This study shows that it is possible to develop a fully biodegradable and bioresorbable bilaminar device with adequate porosity for cell infiltration which can be used as a carrier of ASCs. This device, when associated with ASCs, improves formation of the neo-dermis, stimulates the formation of blood vessels, increases maturation and matrix remodeling, and suppresses the formation of myofibroblasts, helping to reduce fibrosis.

CONCLUSIONS

The PLGA/collagen/ASCs device described here was porous and showed biodegradability compatible with the formation of new skin. Although a foreign body response was observed with all devices tested in this study (Integra, PLGA/collagen, and PLGA/collagen/ASCs), the response was less marked in PLGA/collagen/ASC samples, probably because of the presence of mesenchymal stem cells, which are known to have immunosuppressive properties. Considering the three materials tested, the PLGA/collagen/ASC combination was superior to the others in its ability to stimulate the formation of new skin. This finding suggests that this combination could be useful for regenerating the dermal matrix in individuals with chronic ulcerations and third-degree burns.

Acknowledgments: This research was supported by FAPESP (2011/10928-5)—São Paulo/Brazil, Pontifical University of São Paulo (PUCSP), and CAPES (PNPD20131505). The authors thank the technicians of the Faculty of Mechanical Engineering—University of Campinas—São Paulo (Unicamp) and our team at the Biomaterials Laboratory at PUCSP.

REFERENCES

- Li X, Meng X, Wang X, et al. Human acellular dermal matrix allograft: a randomized, controlled human trial for the long-term evaluation of patients with extensive burns. *Burns* 2015;41:689–99.
- Shen Y, Song H, Papa A, et al. Acellular hydrogel for regenerative burn wound healing: translation from a porcine model. *J Invest Dermatol* 2015;doi: 10.1038/jid.2015.182.
- Freyman TM, Yannas IV, Gibson LJ. Cellular materials as porous scaffolds for tissue engineering. *Prog Mater Sci* 2001;46:273–82.
- Caliari-Oliveira C, Yaochite JN, Ramalho LN, et al. Xenogeneic mesenchymal stromal cells improve wound healing and modulate the immune response in an extensive burn model. *Cell Transp* 2015;doi: 10.3727/096368915X6688128.
- Cancedda R, Dozin B, Giannoni P, et al. Tissue engineering and cell therapy of cartilage and bone. *Mater Biol* 2003;22:81–91.
- Adani R, Rossati L, Tarallo L, Corain M. Use of Integra artificial dermis to reduce donor site morbidity after pedicle flaps in hand surgery. *J Hand Surg [Am]* 2014;39:2228–34.
- Lohana P, Hassan S, Watson SB. Integra™ in burns reconstruction: our experience and report of an unusual immunological reaction. *Ann Burns Fire Disasters* 2014;27:17–21.
- Jadlowiec C, Brenes RA, Li X, et al. Stem cell therapy for critical limb ischemia: what can we learn from cell therapy for chronic wounds? *Vascular* 2012;20:284–9.
- Katti DS, Robinson KW, Ko FK, et al. Bioresorbable nanofiber-based systems matrices for wound healing and drug delivery: optimization of fabrication parameters. *J Biomed Mater Res B Appl Biomater* 2004;70:286–96.
- Zuber A, Borowczyk J, Zimolag E, et al. Poly(L-lactide-co-glycolide) thin films can act as autologous cell carriers for skin tissue engineering. *Cell Mol Biol Lett* 2014;19:297–314.
- Van Der Veen VC, Van Der Wal MBA, Van Leeuwen MCE, et al. Biological background of dermal substitutes. *Burns* 2010;36:305–21.
- Metcalfe AD, Ferguson MW. Tissue engineering of replacement skin: the crossroads of biomaterials, wound healing, embryonic development, stem cells and regeneration. *J R Soc Interface* 2007;4:413–37.
- Yannas IV, Burke JF. Design of an artificial skin. I. Basic design principles. *J Biomed Mater Res* 1980;14:65–81.
- Kim GH, Kim WD. Highly porous 3D nanofiber scaffold using an electrospinning technique. *J Biomed Mater Res B Appl Biomater* 2007;81:104–10.
- Jeremias TS, Machado RG, Visoni SBC, et al. Dermal substitutes support the growth of human skin-derived mesenchymal stromal cells: potential tool for skin regeneration. *PLoS ONE* 2014;9:e89542.
- Balaji S, Keswani SG, Crombleholme TM. The role of mesenchymal stem cells in the regenerative wound healing phenotype. *Adv Wound Care (New Rochelle)* 2012;1:159–65.
- Markeson D, Pleat JM, Sharpe JR, et al. Scarring, stem cells, scaffolds and skin repair. *J Tissue Eng Regen Med* 2013;9:649–68.
- Wang XQ, Kravchuk O, Winterford C, et al. The correlation of in vivo burn scar contraction with the level of α -smooth muscle actin expression. *Burns* 2011;37:1367–77.
- Shi HX, Lin C, Lin BB, et al. The anti-scar effects of basic fibroblast growth factor on wound repair in vitro and in vivo. *PLoS ONE* 2013;8:e59966.
- Rahmani-Neishaboore E, Jallili R, Hartwell R, et al. Topical application of a film-forming emulgel dressing that controls the release of stratifin and acetylsalicylic acid and improves/prevents hypertrophic scarring. *Wound Repair Regen* 2013;21:55–65.
- Motta AC. Síntese e caracterização do poli(L-ácido láctico)-PLLA e poli(L-ácido láctico-co-ácido glicólico)-PLGA e estudo da degradação in vitro. Thesis, Campinas, UNICAMP, 2002.
- Koren R, Yaniv E, Kristt D, et al. Capsular collagen staining of follicular thyroid neoplasms by picosirius red: role in differential diagnosis. *Acta Histochem* 2001;103:151–7.
- Sun X, Cheng L, Zhu W, et al. Use of ginsenoside Rg3-loaded electrospun PLGA fibrous membranes as wound cover induces healing and inhibits hypertrophic scar formation of the skin. *Colloids Surf B Biointerfaces* 2014;115:61–70.
- Fu X, Fang L, Li H, et al. Adipose tissue extract enhances skin wound healing. *Wound Repair Regen* 2007;15:540–8.
- Pan JF, Liu NH, Sun H, Xu F. Preparation and characterization of electrospun PLCL/Poloxamer nanofibers and dextran/gelatin hydrogels for skin tissue engineering. *PLoS ONE* 2014;18:e112885.
- Wu L, Ding J. In vitro degradation of three-dimensional porous poly(D,L-lactide-co-glycolide) scaffolds for tissue engineering. *Biomaterials* 2004;25:5821–30.
- Motta AC, Duek EAR. Synthesis, characterization, and “in vitro” degradation of poly(L-lactic acid-co-glycolic acid), PLGA. *Revista Matéria* 2006;11:340–50.
- Félix Lanao RP, Jonker AM, Wolke JG, et al. Physicochemical properties and applications of poly(lactic-co-glycolic acid) for use in bone regeneration. *Tissue Eng Part B Rev* 2013;19:380–90.
- Song J, Zhang P, Cheng L, et al. Nano-silver in situ hybridized collagen scaffolds for regeneration of infected full-thickness burn skin. *J Mater Chem B* 2015;3:4231–41.
- Yahyouché A, Zhidao X, Czernuszka JT, et al. Macrophage-mediated degradation of crosslinked collagen scaffolds. *Acta Biomater* 2011;7:278–86.
- Puppi D, Chiellini F, Piras AM, et al. Polymeric materials for bone and cartilage repair. *Prog Polym Sci* 2010;35:403–40.
- Guo R, Xu S, Ma L, et al. The healing of full-thickness burns treated by using plasmid DNA encoding vegf-165 activated collagen-chitosan dermal equivalents. *Biomaterials* 2011;32:1019–31.

33. O'Brien FJ, Harley BA, Yannas IV, et al. The effect of pore size on cell adhesion in collagen-GAG scaffolds. *Biomaterials* 2005;26:433–41.
34. Szot CS, Buchanan CF, Freeman JW, Rylander MN. 3D in vitro bioengineered tumors based on collagen I hydrogels. *Biomaterials* 2011;32:7905–12.
35. Colom A, Galgoczy R, Almendros I, et al. Oxygen diffusion and consumption in extracellular matrix gels: implications for designing three-dimensional cultures. *J Biomed Mater Res A* 2014;102:2776–84.
36. Sullivan TP, Eaglstein WH, Davis SC, Mertz P. The pig as a model for human wound healing. *Wound Repair Regen* 2001;9:66–76.
37. Briscoe DM, Dharnidharka VR, Isaacs C, et al. The allogeneic response to cultured human skin equivalent in the hu-PBL-SCID mouse model of skin rejection. *Transplantation* 1999;67:1590–9.
38. Lynn AK, Yannas IV, Bonfield W. Antigenicity and immunogenicity of collagen. *J Biomed Mater Res B Appl Biomater* 2004;71:343–54.
39. Browne S, Zeugolis DI, Pandit A. Collagen: finding a solution for the source. *Tissue Eng Part A* 2013;19:1491–4.
40. Chung E, Son Y. Crosstalk between mesenchymal stem cells and macrophages in tissue repair. *Tissue Eng Regen Med* 2014;11:431–8.
41. Zonari A, Martins TM, Paula AC, et al. Polyhydroxybutyrate-co-hydroxyvalerate structures loaded with adipose stem cells promote skin healing with reduced scarring. *Acta Biomater* 2015;17:170–81.
42. Lee EY, Xia Y, Kim W-S, et al. Hypoxia-enhanced wound-healing function of adipose derived stem cells: increase in stem cell proliferation and up-regulation of VEGF and bFGF. *Wound Repair Regen* 2009;17:540–7.
43. Jiang D, Qi Y, Walker NG, et al. The effect of adipose tissue derived MSCs delivered by a chemically defined carrier on full thickness cutaneous wound healing. *Biomaterials* 2013;34:2501–15.
44. Ren G, Zhang L, Zhao X, et al. Mesenchymal stem cell-mediated immunosuppression occurs via concerted action of chemokines and nitric oxide. *Cell Stem Cell* 2008;2:141–50.
45. Leonardi D, Oberdoerfer D, Fernandes MC, et al. Mesenchymal stem cells combined with an artificial dermal substitute improve repair in full-thickness skin wounds. *Burns* 2012;38:1143–50.
46. Liu YL, Liu WH, Sun J, et al. Mesenchymal stem cell-mediated suppression of hypertrophic scarring is p53 dependent in a rabbit ear model. *Stem Cell Res Ther* 2014;5:136.
47. Liu S, Jiang L, Li H, et al. Mesenchymal stem cells prevent hypertrophic scar formation via inflammatory regulation when undergoing apoptosis. *J Invest Dermatol* 2014;134:2648–57.
48. Gurtner GC, Werner S, Barrandon Y, Longaker MT. Wound repair and regeneration. *Nature* 2008;453:314–21.